

# Isospin splitting of nucleon effective mass and shear viscosity of nuclear matter

Jun Xu\*

Shanghai Institute of Applied Physics, Chinese Academy of Sciences, Shanghai 201800, China  
and Kavli Institute for Theoretical Physics China, CAS, Beijing 100190, China

(Received 20 January 2015; published 2 March 2015)

Based on an improved isospin- and momentum-dependent interaction, I have studied the qualitative effect of isospin splitting of nucleon effective mass on the specific shear viscosity of neutron-rich nuclear matter from a relaxation time approach. It is seen that for  $m_n^* > m_p^*$ , the relaxation time of neutrons is smaller, and the neutron flux between flow layers is weaker, leading to a smaller specific shear viscosity of neutron-rich matter compared to the case for  $m_n^* < m_p^*$ . The effect is larger in nuclear matter at higher densities, lower temperatures, and larger isospin asymmetries, but it does not affect the behavior of the specific shear viscosity much near nuclear liquid-gas phase transition.

DOI: [10.1103/PhysRevC.91.037601](https://doi.org/10.1103/PhysRevC.91.037601)

PACS number(s): 21.65.-f, 64.10.+h, 51.20.+d

Understanding the basic strong interaction and the properties of nuclear matter is the main purpose of nuclear physics. The knowledge of transport properties of the hot dense matter is important in understanding the dynamics in heavy-ion collision experiments as well as the properties of protoneutron stars. The quark-gluon plasma (QGP) produced in ultrarelativistic heavy-ion collisions is believed to be a nearly ideal fluid and has a very small specific shear viscosity  $\eta/s$  [1–4], i.e., the ratio of the shear viscosity  $\eta$  to the entropy density  $s$ . It has been further found that the  $\eta/s$  decreases with increasing temperature in the hadronic phase while increases with increasing temperature in QGP, resulting in a minimum value at the temperature of hadron-quark phase transition [5,6]. At even lower temperatures, the  $\eta/s$  of nuclear matter with nucleon degree of freedom has been investigated from the relaxation time approach [7–9] and transport model studies [10–13]. Similar to the behavior near hadron-quark phase transition, the  $\eta/s$  also shows a minimum in the vicinity of nuclear liquid-gas phase transition from various approaches [11–16]. Since the correlation between the elliptic flow and the specific shear viscosity seems to be a general feature in not only relativistic [3] but also intermediate-energy heavy-ion collisions [17], it might be promising to measure the  $\eta/s$  experimentally, meanwhile providing an alternative way of searching for nuclear liquid-gas phase transition in heavy-ion collisions at intermediate energies in the future.

In my previous studies, the specific shear viscosity of neutron-rich matter was investigated based on an isospin- and momentum-dependent interaction [9,16]. Recently, this interaction has been further improved [18], providing the possibility of studying more flexibly detailed isovector properties of nucleon interaction, such as the neutron-proton effective mass splitting. The interest was inspired by the recent experimental data of double neutron/proton ratio from the National Superconducting Cyclotron Laboratory, which seems to favor a smaller neutron effective mass than proton based on the calculation using an improved quantum molecular dynamics model [19]. However, the well-known Lane

potential, representing the nuclear symmetry potential, i.e., the difference between the mean-field potential of neutrons and protons, decreases with increasing nucleon energy, leading to a larger neutron effective mass than proton [20]. To explore the possible uncertainty of neutron-proton effective mass splitting on the  $\eta/s$  of hot neutron-rich nuclear matter, I extend my study of the specific shear viscosity with the improved isospin- and momentum-dependent interaction (ImMDI) in this Brief Report.

The single-nucleon mean-field potential of the ImMDI interaction is written as [18]

$$\begin{aligned}
 U_\tau(\rho, \delta, \vec{p}) = & A_u \frac{\rho_{-\tau}}{\rho_0} + A_l \frac{\rho_\tau}{\rho_0} \\
 & + B \left( \frac{\rho}{\rho_0} \right)^\sigma (1 - x\delta^2) - 4\tau x \frac{B}{\sigma + 1} \frac{\rho^{\sigma-1}}{\rho_0^\sigma} \delta \rho_{-\tau} \\
 & + \frac{2C_l}{\rho_0} \int d^3 p' \frac{f_\tau(\vec{p}')}{1 + (\vec{p} - \vec{p}')^2 / \Lambda^2} \\
 & + \frac{2C_u}{\rho_0} \int d^3 p' \frac{f_{-\tau}(\vec{p}')}{1 + (\vec{p} - \vec{p}')^2 / \Lambda^2}, \quad (1)
 \end{aligned}$$

where  $\tau = 1(-1)$  for neutrons (protons) is the isospin index,  $\rho_n$  and  $\rho_p$  are number densities of neutrons and protons, respectively,  $\delta = (\rho_n - \rho_p)/\rho$  is the isospin asymmetry, with  $\rho = \rho_n + \rho_p$  being the total number density, and  $f_\tau(\vec{p})$  is the phase-space distribution function. The  $x$  parameter is used to mimic the slope parameter of the symmetry energy at saturation density  $\rho_0$ , while additional two parameters  $y$  and  $z$  are introduced to adjust the symmetry potential  $U_{\text{sym}}$  at infinitely large nucleon momentum and the value of symmetry energy  $E_{\text{sym}}$  at saturation density, respectively, and they enter the functional through the relations

$$A_l(x, y) = A_{l0} + y + x \frac{2B}{\sigma + 1}, \quad (2)$$

$$A_u(x, y) = A_{u0} - y - x \frac{2B}{\sigma + 1}, \quad (3)$$

$$C_l(y, z) = C_{l0} - 2(y - 2z) \frac{p_{f0}^2}{\Lambda^2 \ln[(4p_{f0}^2 + \Lambda^2)/\Lambda^2]}, \quad (4)$$

\*xujun@sinap.ac.cn

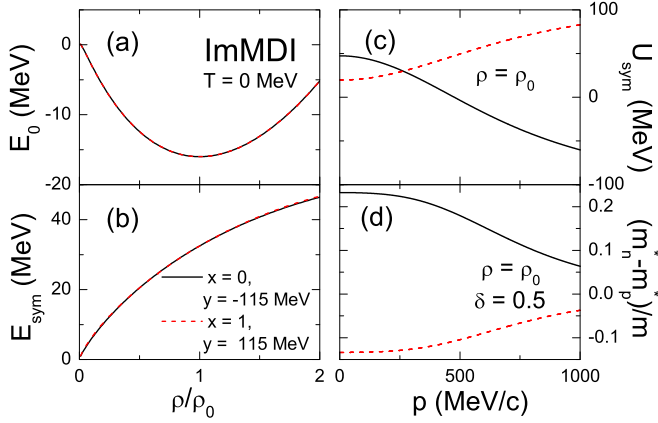


FIG. 1. (Color online) Binding energy in symmetric nuclear matter (a), symmetry energy (b), symmetry potential at saturation density (c), and relative neutron-proton effective mass splitting (d) in nuclear matter at saturation density and isospin asymmetry  $\delta = 0.5$  from the two parameter sets based on the ImMDI interaction.

$$C_u(y, z) = C_{u0} + 2(y - 2z) \frac{p_{f0}^2}{\Lambda^2 \ln[(4p_{f0}^2 + \Lambda^2)/\Lambda^2]}, \quad (5)$$

where  $p_{f0}$  is the nucleon Fermi momentum in symmetric nuclear matter at saturation density. The values of parameters  $A_{l0}$ ,  $A_{u0}$ ,  $B$ ,  $C_{l0}$ ,  $C_{u0}$ ,  $\Lambda$ , and  $\sigma$  as well as the corresponding macroscopic properties of nuclear matter from the ImMDI interaction can be found in Ref. [18].

The values of  $x$ ,  $y$ , and  $z$  do not affect the isoscalar properties of nuclear matter, and the binding energy in symmetric nuclear matter is shown in Fig. 1(a). The parameter  $z$  is set to be 0 in the present study, while  $x$  and  $y$  change, respectively, the magnitude and the momentum dependence of the symmetry potential, and they both contribute to the density dependence of the symmetry energy. With different combinations of  $x$  and  $y$ , one can get very similar density dependence of symmetry energy but different momentum dependence of the symmetry potential, or equivalently, the isospin splittings of nucleon effective mass, as can be seen from Figs. 1(b)–1(d), with the nucleon effective mass calculated from

$$\frac{m_\tau^*}{m} = \left( 1 + \frac{m}{p} \frac{dU_\tau}{dp} \right)^{-1}. \quad (6)$$

The parameter sets  $[(x = 0), (y = -115 \text{ MeV})]$  with  $m_n^* > m_p^*$  and  $[(x = 1), (y = 115 \text{ MeV})]$  with  $m_n^* < m_p^*$  are thus chosen in the following study.

I now briefly review the main ingredient of the relaxation time approach used in previous studies [9,16]. The shear viscosity is calculated by assuming that in the uniform nuclear system there exists a static flow field in the  $z$  direction with flow gradient in the  $x$  direction. The shear force, which is related to the nucleon flux as well as the momentum exchange between flow layers, is proportional to the flow gradient, and the proportionality coefficient, i.e., the shear viscosity, turns

out to be [9]

$$\eta = \sum_\tau -\frac{d}{(2\pi)^3} \int \tau_\tau(p) \frac{p_z^2 p_x^2}{p m_\tau^*} \frac{dn_\tau}{dp} dp_x dp_y dp_z. \quad (7)$$

In the above,  $d = 2$  is the spin degeneracy,  $p = \sqrt{p_x^2 + p_y^2 + p_z^2}$  is the nucleon momentum, and  $n_\tau$  is the local momentum distribution

$$n_\tau(\vec{p}) = f_\tau(\vec{p})/d = \frac{1}{\exp[(\frac{p^2}{2m} + U_\tau(\vec{p}) - \mu_\tau)/T] + 1} \quad (8)$$

with  $\mu_\tau$  and  $T$  being the chemical potential and the temperature, respectively.  $p_x/m_\tau^*$  is the nucleon velocity between flow layers.  $\tau_\tau(p)$  is the relaxation time for a nucleon with isospin  $\tau$  and momentum  $p$ , and it can be further expressed as

$$\frac{1}{\tau_\tau(p)} = \frac{1}{\tau_\tau^{\text{same}}(p)} + \frac{1}{\tau_\tau^{\text{diff}}(p)}, \quad (9)$$

with  $\tau_\tau^{\text{same(diff)}}(p)$  being the average collision time for a nucleon with isospin  $\tau$  and momentum  $p$  when colliding with other nucleons of same (different) isospin. For more detailed derivations and the expressions of the relaxation time, I refer the reader to Ref. [9]. The relaxation time depends not only on the medium properties such as the density, temperature, and isospin asymmetry, but on the nucleon-nucleon scattering cross section as well. The free-space proton-proton and neutron-proton cross sections ( $\sigma_{NN}$ ) are taken as the parameterized forms from Ref. [21], while the in-medium cross section is modified by the effective mass through [22]

$$\sigma_{NN}^{\text{medium}} = \sigma_{NN} \left( \frac{\mu_{NN}^*}{\mu_{NN}} \right)^2, \quad (10)$$

where  $\mu_{NN}$  ( $\mu_{NN}^*$ ) is the free-space (in-medium) reduced mass of colliding nucleons. The reduced mass scaling of the in-medium cross section comes from the fact that the differential cross section is inversely proportional to the relative velocity between the two colliding nucleons [23], while the difference between the scattering  $T$  matrix in free space and in the nuclear medium is neglected in the present qualitative study.

Figure 2 displays the total relaxation time and those for nucleon scatterings with same or different isospins. As expected, all relaxation times are larger with in-medium cross sections compared to the results with those in free space. In neutron-rich nuclear matter, the scatterings are more frequent for neutron-neutron than for proton-proton, and protons have more chance to collide with nucleons of a different isospin than neutrons. The total neutron relaxation time dominates the shear viscosity due to the sharper neutron momentum distribution in neutron-rich nuclear matter as can be seen from Eq. (7), and it is larger for  $m_n^* < m_p^*$  than for  $m_n^* > m_p^*$  as a result of the isospin-dependent modification from the in-medium effective mass, while the difference of the total neutron relaxation time for different isospin effective mass splittings is smaller with free-space cross sections.

The extensive results of the specific shear viscosity in nuclear matter of isospin asymmetry  $\delta = 0.5$  at various densities and temperatures are shown in Fig. 3. Although the

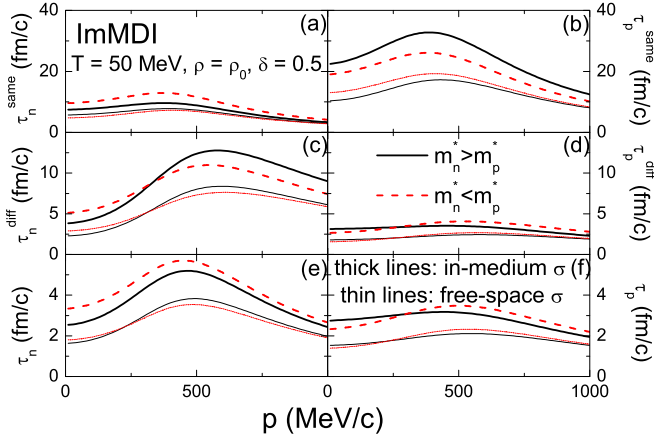


FIG. 2. (Color online) Momentum dependence of the total relaxation time and that for a nucleon to collide with other ones of same or different isospin in nuclear matter at saturation density and isospin asymmetry of  $\delta = 0.5$  using free-space or in-medium nucleon-nucleon scattering cross sections.

momentum occupation probability  $n_\tau(\vec{p})$  at finite temperature depends on the neutron-proton effective mass splitting [18], the difference of the entropy density, which is calculated from

$$s = - \sum_\tau d \int [n_\tau \ln n_\tau + (1 - n_\tau) \ln(1 - n_\tau)] \frac{d^3 p}{(2\pi)^3}, \quad (11)$$

turns out to be small between  $m_n^* > m_p^*$  and  $m_n^* < m_p^*$ . Despite of the similar relaxation time for different isospin splittings of nucleon effective mass using free-space cross sections, a larger neutron effective mass leads to smaller neutron fluxes between flow layers, reducing the shear viscosity as can be seen from Eq. (7). I note that this is a robust feature even if a naive mean-free-path formula is used. The isospin-dependent modification for the in-medium cross sections further enhances the difference of the specific shear viscosity between  $m_n^* > m_p^*$

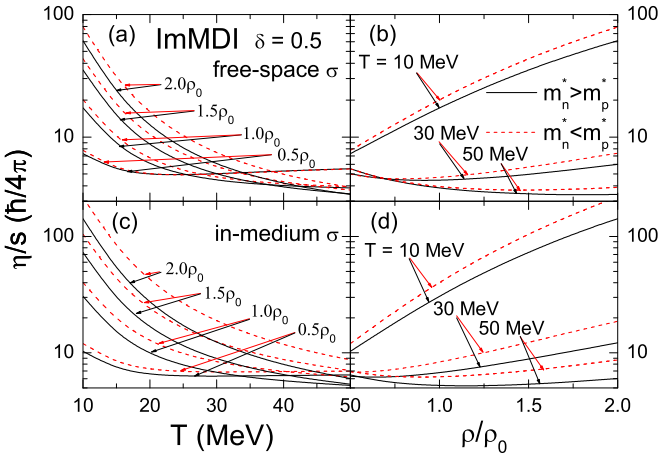


FIG. 3. (Color online) Specific shear viscosity with free-space [(a), (b)] and in-medium [(c), (d)] cross sections in nuclear matter of isospin asymmetry  $\delta = 0.5$  at different densities and temperatures for  $m_n^* > m_p^*$  and  $m_n^* < m_p^*$ .

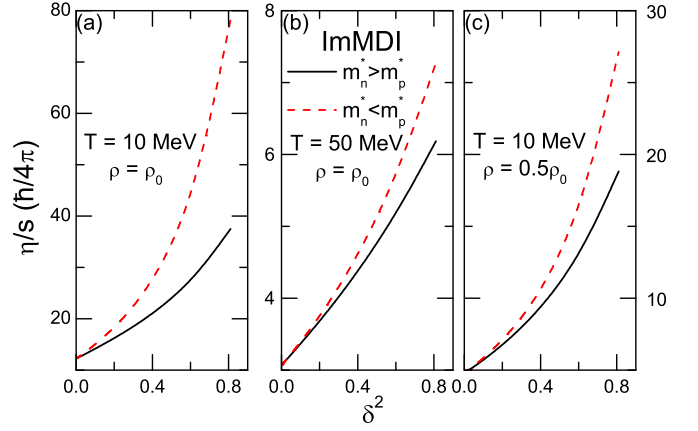


FIG. 4. (Color online) Isospin asymmetry dependence of the specific shear viscosity in nuclear matter at different temperatures and densities for  $m_n^* > m_p^*$  and  $m_n^* < m_p^*$ .

and  $m_n^* < m_p^*$  by giving a smaller relaxation time for neutrons in the former case, as discussed in Fig. 2. In addition, one sees that the difference is larger at higher densities and lower temperatures when the relative isospin splitting of nucleon effective mass is generally stronger [18].

The dependence of the specific shear viscosity on the isospin asymmetry is displayed in Fig. 4 at different temperatures and densities. It is seen that  $\eta/s$  increases with increasing isospin asymmetry  $\delta$  faster than a parabolic relation especially for  $m_n^* < m_p^*$ , and it increases even faster at higher densities or lower temperatures. The effect discussed here is quite relevant for the evolution of hot neutron stars with a large neutron excess.

During the liquid-gas phase transition (LGPT) in nuclear matter, each phase satisfying the Gibbs condition [24,25] has its own volume fraction. The thin lines in Figs. 5(a)–5(c) show the evolution of the entropy when the nuclear matter of isospin asymmetry  $\delta = 0.5$  is heated at different external

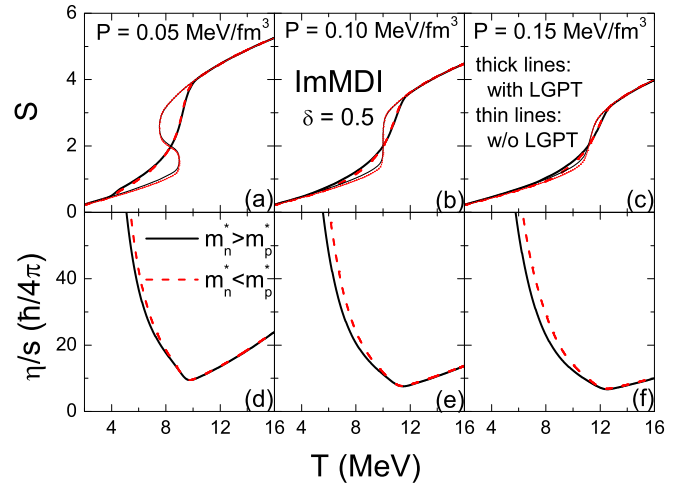


FIG. 5. (Color online) Temperature evolution of the entropy (upper panels) and specific shear viscosity (lower panels) in the presence of nuclear liquid-gas phase transition (LGPT) at fixed external pressure  $P = 0.05$  [(a), (d)],  $0.10$  [(b), (e)], and  $0.15$   $\text{MeV}/\text{fm}^3$  [(c), (f)] and isospin asymmetry  $\delta = 0.5$  for  $m_n^* > m_p^*$  and  $m_n^* < m_p^*$ .

pressures. If the occurrence of nuclear LGPT is taken into account, the entropy evolution will follow the thick lines, with the overall entropy density from that in each phase weighted by the volume fraction. In infinite nuclear matter the total shear viscosity can also be calculated from that in each phase weighted by the volume fraction [16], and the temperature evolution of the specific shear viscosity is shown in Figs. 5(d)–5(f). A minimum value of  $\eta/s$  is seen at a higher temperature with increasing pressure, and this value is also smaller at a larger external pressure. The isospin splitting of nucleon effective mass has small effects on the entropy evolution. The specific shear viscosity is smaller for  $m_n^* > m_p^*$  than for  $m_n^* < m_p^*$  at lower temperatures (higher densities) in the liquid phase side, but the difference is negligible at higher temperatures (lower densities) in the gas phase side. Moreover, the minimum point of  $\eta/s$  is not affected by the isospin splitting of the nucleon effective mass. This general feature, which is not sensitive to detailed behaviors of nuclear interaction, might be helpful in searching for the occurrence of nuclear LGPT in low- and intermediate-energy heavy-ion collisions, if people find ways to measure the specific shear viscosity there.

In summary, the specific shear viscosity with different isospin splittings of nucleon effective mass has been studied

in neutron-rich nuclear matter based on an improved isospin- and momentum-dependent interaction. Qualitatively, it is seen that the specific shear viscosity is larger for  $m_n^* < m_p^*$  than for  $m_n^* > m_p^*$ , and the difference is more obvious at higher densities, lower temperatures, and larger isospin asymmetries. This is due to different neutron fluxes between flow layers as well as the isospin-dependent modification to the in-medium nucleon-nucleon cross sections. On the other hand, the behavior of the specific shear viscosity near nuclear liquid-gas phase transition remains robust and seems to be insensitive to the detailed nuclear interaction. The study may be helpful in understanding the transport property of the hot neutron-rich nuclear matter produced in heavy-ion collision experiments as well as that in hot neutron stars.

This work was supported by the Major State Basic Research Development Program (973 Program) in China under Contract Nos. 2015CB856904 and 2014CB845401, the National Natural Science Foundation of China under Grant Nos. 11475243 and 11421505, the “100-talent plan” of Shanghai Institute of Applied Physics under Grant No. Y290061011 from the Chinese Academy of Sciences, and the “Shanghai Pujiang Program” under Grant No. 13PJ1410600.

- 
- [1] A. Peshier and W. Cassing, *Phys. Rev. Lett.* **94**, 172301 (2005).
  - [2] A. Majumder, B. Müller, and X. N. Wang, *Phys. Rev. Lett.* **99**, 192301 (2007).
  - [3] H. Song, S. A. Bass, U. Heinz, T. Hirano, and C. Shen, *Phys. Rev. Lett.* **106**, 192301 (2011).
  - [4] B. Schenke, S. Jeon, and C. Gale, *Phys. Rev. Lett.* **106**, 042301 (2011).
  - [5] L. P. Csernai, J. I. Kapusta, and L. D. McLerran, *Phys. Rev. Lett.* **97**, 152303 (2006).
  - [6] R. A. Lacey *et al.*, *Phys. Rev. Lett.* **98**, 092301 (2007).
  - [7] P. Danielewicz, *Phys. Lett. B* **146**, 168 (1984).
  - [8] L. Shi and P. Danielewicz, *Phys. Rev. C* **68**, 064604 (2003).
  - [9] J. Xu, *Phys. Rev. C* **84**, 064603 (2011); *Nucl. Sci. Tech.* **24**, 050514 (2013).
  - [10] S. X. Li, D. Q. Fang, Y. G. Ma, and C. L. Zhou, *Phys. Rev. C* **84**, 024607 (2011).
  - [11] C. L. Zhou *et al.*, *Europhys. Lett.* **98**, 66003 (2012).
  - [12] C. L. Zhou, Y. G. Ma, D. Q. Fang, and G. Q. Zhang, *Phys. Rev. C* **88**, 024604 (2013).
  - [13] D. Q. Fang, Y. G. Ma, and C. L. Zhou, *Phys. Rev. C* **89**, 047601 (2014).
  - [14] J.-W. Chen, Y.-H. Li, Y.-F. Liu, and E. Nakano, *Phys. Rev. D* **76**, 114011 (2007).
  - [15] S. Pal, *Phys. Rev. C* **81**, 051601(R) (2010).
  - [16] J. Xu *et al.*, *Phys. Lett. B* **727**, 244 (2013).
  - [17] C. L. Zhou *et al.*, *Phys. Rev. C* **90**, 057601 (2014).
  - [18] J. Xu, L. W. Chen, and B. A. Li, *Phys. Rev. C* **91**, 014611 (2015); L. W. Chen and B. A. Li, a note of an improved MDI interaction for transport model simulations of heavy ion collisions, Texas A&M University-Commerce, 2010 (unpublished).
  - [19] D. D. S. Coupland *et al.*, [arXiv:1406.4546](https://arxiv.org/abs/1406.4546) [nucl-th].
  - [20] B. A. Li, *Phys. Rev. C* **69**, 064602 (2004).
  - [21] S. K. Charagi and S. K. Gupta, *Phys. Rev. C* **41**, 1610 (1990).
  - [22] B. A. Li and L. W. Chen, *Phys. Rev. C* **72**, 064611 (2005).
  - [23] V. R. Pandharipande and S. C. Pieper, *Phys. Rev. C* **45**, 791 (1992).
  - [24] H. Müller and B. D. Serot, *Phys. Rev. C* **52**, 2072 (1995).
  - [25] J. Xu *et al.*, *Phys. Lett. B* **650**, 348 (2007).